Original Research

Safety Evaluation of a 405-nm LED Device for Direct Antimicrobial Treatment of the Murine Brain

Colleen E Thurman,[1–3,*] Anantharaman Muthuswamy,[1,3] Mark M Klinger,[1,2] and Gordon S Roble[1,2,4]

Antimicrobial resistance is a growing problem in human medicine that extends to biomedical research. Compared with chemical-based therapies, light-based therapies present an alternative to traditional pharmaceuticals and are less vulnerable to acquired bacterial resistance. Due to immunologic privilege and relative tissue sensitivity to topical antibiotics, the brain poses a unique set of difficulties with regard to antimicrobial therapy. This study focused on 405-nm 'true violet' light—which has been shown to kill multiple clinically relevant bacterial species in vitro yet leave mammalian cells unscathed—and its effect on the murine brain. We built a 405-nm LED array, validated its power and efficacy against a clinical bacterial isolate in vitro, and then, at the time of craniotomy, treated mice with various doses of 405-nm light (36, 45, and 54 J/cm²). The selected doses caused no behavioral derangements postoperatively or any observable brain pathology as determined postmortem by histologic evaluation and immunofluorescence staining for caspase 3 and glial fibrillary acidic protein, markers of apoptosis and necrosis. True-violet light devices may present an inexpensive refinement to current practices for maintaining open craniotomy sites or reducing bacterial loads in contaminated surgical sites.

Antimicrobial treatment in open cranial surgery sites presents a persistent problem in neurologic and psychologic research.[1,3] Topical application of chemical antiseptics and antibiotics has limited usefulness due to the sensitivity of brain tissue, especially when dura has been removed.[1,2,3,17] Systemic antibiotics often do not sufficiently control these infections because of the blood–brain barrier.[1,3,11] Human patients often require a second surgical procedure to address localized infections after craniotomy.[11] In addition, biofilm-forming organisms present a particular challenge in neuroscience research because their sensitivity to antibiotics in vitro often does not accurately predict the efficacy of the same drugs for controlling infection in a recording chamber or other craniotomy site.[17,29] Novel antimicrobial treatment modalities, including phototherapy, present an exciting area of medical exploration because they provide a means to access privileged sites and to circumvent antimicrobial resistance to pharmaceutical agents.

Many light-based devices, particularly in the UV range, have been investigated for their antimicrobial properties. Their ability to kill bacterial species—despite the presence of antimicrobial resistance genes—and their effectiveness against diverse organisms make light-based devices extremely valuable for environmental decontamination.[5,12,20,22] However, UV light is harmful to mammalian cells and can induce DNA damage and subsequent cell death or carcinogenesis if used in vivo.[12] Light sources that are lower in energy, such as blue-range visible light (430 to 450 nm), and cold lasers (600 to 900 nm, less than 500 mW) have been investigated for multiple dermatologic uses, wound healing, and pain relief.[15,26] However, evidence is equivocal in regard to their efficacy.[15] True violet light lies between the available blue-light treatment modalities—which are considered safe if not necessarily effective—and UV, which is effective but often unsafe (Figure 1). Like laser diodes, LED transmit a single wavelength of light, but the photons are out of phase (that is, noncoherent), so they deliver energy over a greater area per unit time, although often at lower power, than do coherent photons (Figure 1).[6] At various doses in vitro, true violet (that is, 405 nm) LED devices are bactericidal but permissive to mammalian cell growth.[5,10,12,18,19,21–23] Devices that deliver light of similar spectrum have decreased fungal burdens both in vivo and in vitro and killed biofilm-forming bacteria in vivo in an inoculated murine burn model.[9,27,32] In addition, 405-nm violet light has been used safely in microglial culture, making this wavelength a good candidate for direct in vivo treatment of the brain.[7]

Bacteria of multiple clinically relevant genera, including biofilm-forming organisms, are more sensitive to light therapy (phototherapy) in the blue-violet range than mammalian cells.[9,22] This difference is thought to be due to the inherent photosensitivity of cytoplasmic chromophores, which mammalian cells lack.[9,14] Similar antimicrobial studies have been performed using photodynamic therapy, where exogenous photosensitizers are added for efficacy to a light-based therapy.[9] Studies of photodynamic therapy using visible light have shown that bacteria do not develop resistance over multiple (that is, as many as 20) treatments, but similar studies into resistance development have not been performed for nonpotentiated visible-spectrum therapies.[9,14] Another study demonstrated that reactive oxygen scavengers protected mammalian cells from damage due

A

Visible Light

Ultraviolet ← | → Infrared

380 nm 770 nm

B

White Light
Multiple wavelengths
Noncoherent

Laser Light
Single wavelength
Coherent

Light Emitting Diode
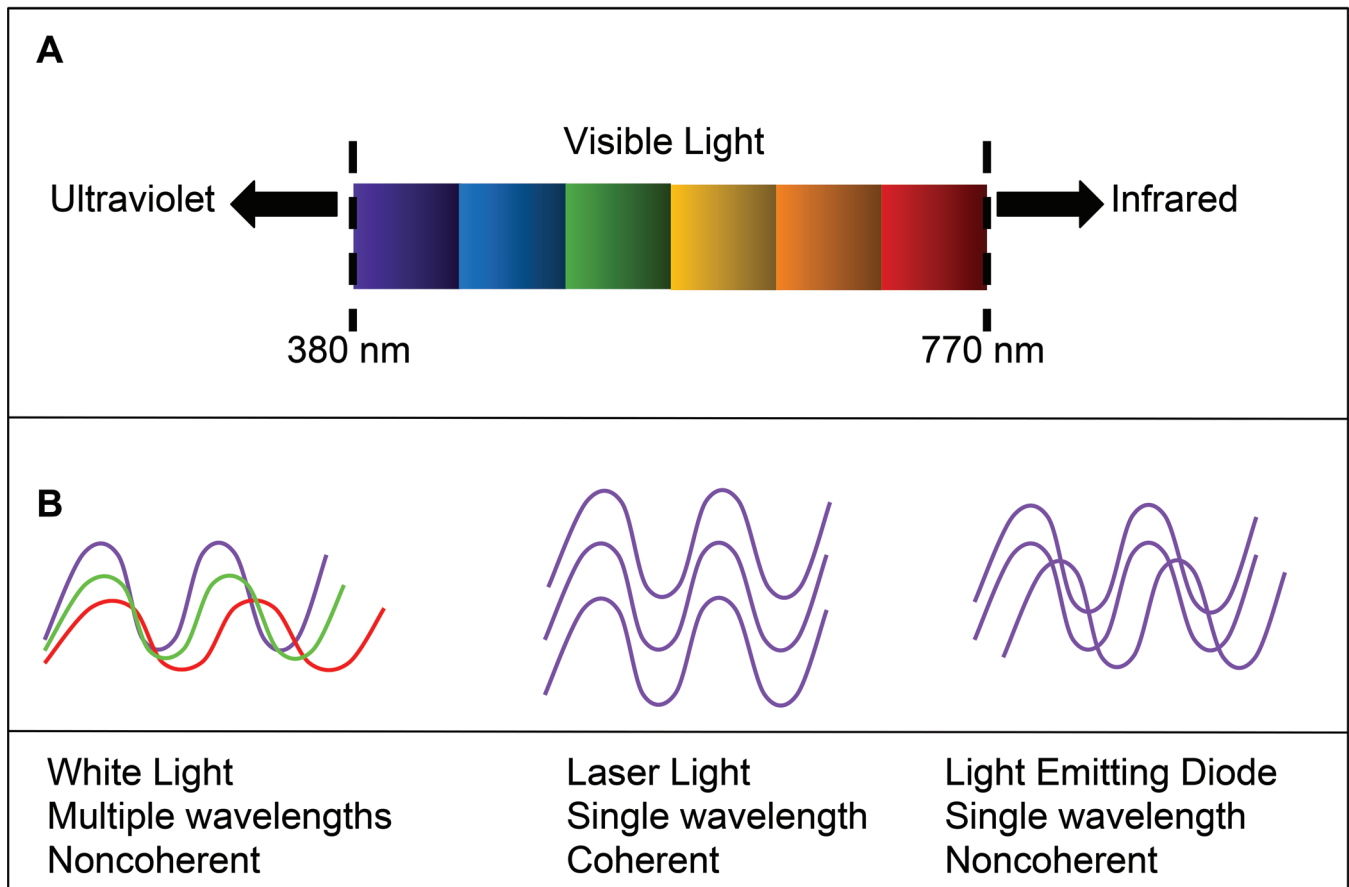Single wavelength
Noncoherent

Figure 1. (A) Wavelength spectrum of visible light. (B) Properties of white light compared with laser and LED light. The monochromaticity of LED makes it a good candidate for directed therapy, despite a lack of coherence. Figure adapted from references 6 and 28, with permission.

to high-dose, visible-light exposure in vitro, even at otherwise cytotoxic doses.[23]

In this study, we built a 405-nm LED array device to treat the brains of live mice after cranial surgery. The device was validated for intensity to determine appropriate distance and time of exposure to deliver doses consistent with published literature. We chose 2 doses (36 and 45 J/cm²) for their published ability to kill bacterial cells yet spare mammalian cells in vitro.[23] We also chose a higher dose, 54 J/cm², because a previous study showed that mammalian cells in vitro could be rescued from damage at that dose due to the presence of reactive oxygen scavengers.[23] We expected all dose levels to be antimicrobial on the basis of previous in vitro and in vivo studies.[9,19,23] Mice underwent craniotomy surgery followed by topical exposure treatment with various doses of 405-nm light. We hypothesized that the 3 tested doses of 405-nm light would not cause significantly greater tissue damage according to histology and immunofluorescence analysis for apoptosis and necrosis markers compared with craniotomy alone.

Materials and Methods

Construction of 405-nm LED light device. A LED array was built by using 9 true-violet (405 nm) solderless LED (Exotic, LEDGroupBuy, St Louis, MO), which were wired in series with 24-AWG solid wire (NTE Electronics, Bloomfield, NJ), driven by a 40-W, 700-mA driver (Inventronics, Hangzhou, China), and attached to a 6-in. heat sink (MakersLED, Ames, IA).

Testing of device power. The dose on the surface of the target was adjusted by changing the time of exposure and distance between the source and target. Irradiance was measured by using an optical power meter (model S310C, Thorlabs, Newton, NJ) at 3 to 6 cm. Three consecutive measurements were made at 3 distances from the sensor, with the sensor held in parallel to the heat sink. Unit calculations accounting for the sensor surface area (0.7 cm²) were performed to convert dosing to intensity units (mW/cm²). Linear and power regressions of measurements (Excel, Microsoft, Redmond, WA) were used to assess the adherence of the observed values to the inverse-squares law— the expected relationship between irradiance and distance of the sensor. Tissue surface temperature ($n = 3$) after exposure to the device (54 J/cm²) was measured by using a liquid-in-glass thermometer at a distance of 3 cm.

In vitro validation of antimicrobial light device. A pure culture of *Enterobacter cloacae* was isolated from a cephalic recording chamber in an NHP by using tryptic soy agar in culture dishes (100×15 mm; Fisher Scientific, Pittsburgh, PA). and organism identity was confirmed (IDEXX Laboratories, North Grafton, MA). Bacteria were propagated by incubation (model 132000, Boekel Scientific, Feasterville-Trevose, PA) at 37 °C in tryptic soy broth. Both tryptic soy agar and tryptic soy broth were made according to published specifications (ATCC, Manassas, VA).

Bacteria were serially diluted in lactated Ringer solution (Hospira Worldwide, Lake Forest, IL) after 24 h of incubation, which provided physiologic electrolyte balance without the need for additional nutrients for continued growth. Dilutions were plated on tryptic soy agar (0.5 mL per plate) and incubated for 24 h at 37 °C, and colonies on plates with 30 to 1000 cfu were counted.

Dilutions that yielded 10⁶ and 10⁷ cfu/mL were treated with 36, 45, and 54 J/cm² doses of 405-nm light; these doses have

been shown to be bactericidal but preserve mammalian cell viability in the presence of oxygen scavengers.[23] Due to attenuation by the solution, a concentration of 10^7 cfu/mL likely has the maximal turbidity at which this device will be effective to a depth of 7 mm.[19] 5-mL aliquots of solution were constantly agitated in borosilicate glass test tubes (7 mL, 10×75 mm; DWK Life Sciences, Millville, NJ) and 15×100 mm culture dishes at 3cm distance and drawing off 0.5ml at time 0, and after delivery of doses of 36 J/cm², 45 J/cm², and 54 J/cm². Plates were incubated for 24 h, and colonies were counted as described earlier. Bacterial kill was evaluated statistically according to 2-factor ANOVA by comparing the ratio $N:N_0$ (the number of surviving cfu/mL relative to the initial number of cfu/mL) as a factor of light dose by using R statistical software.[25] Tukey posthoc testing was used to assess the difference in effect between different light doses.

Animals. The subjects were 84 (n = 7 per group) experimentally naive male and female adult (age, 6 wk to 6 mo) C57Bl/6J (The Jackson Laboratory, Bar Harbor, ME) and C57Bl/6CRL (Charles River Laboratories, Wilmington, MA) mice produced from inhouse breeding at New York University of fewer than 10 generations and housed in OptiMice caging (484 cm² wedge-shaped cages; AnimalCare Systems, Centennial, CO) under standard conditions. The sample size was adapted from a study assessing histologic changes, apoptosis, and astrogliosis after traumatic brain injury in rats; the analysis using similar histologic markers achieved statistical significance.[4] Mice automatically received 5-µm–filtered water (Edstrom Industries, Palmyra, PA), 1/4-in. corncob bedding (Bed -o'Cobs, Andersons Lab Bedding, Maumee, OH), autoclaved nesting tissue (BioServ, Flemington, NJ), a Shepherd Shack (SSP, Watertown PA), and free-choice feed (diet 5001, LabDiet, St Louis, MO). The room was maintained on a 12:12-h light:dark cycle under fluorescent lighting and had 10 air changes hourly. The holding room was ventilated with 95% filtered outside air at 10 air changes hourly, the temperature is maintained at 72 ± 2 °F (21.5 ± 1.0 °C), relative humidity is maintained between 30% and 70%. Cages were changed once every 2 wk. Mice were group-housed (maximum, 4 animals per cage) in single-sex groups unless fighting was observed. Animals were free of ectromelia virus, enzootic diarrhea of infant mice virus, lymphocytic choriomeningitis virus, mouse hepatitis virus, mouse norovirus, mouse parvovirus, minute virus of mice, polyoma virus, reovirus 3, mouse thymoma virus, Sendai virus, *Mycoplasma pulmonis*, *Helicobacter* spp., *Myocoptes* spp., *Radfordia* spp., *Myobia* spp., *Aspicularis tetraptera*, and *Syphacia muris*. All animal work was performed in an AAALAC-accredited facility in accordance with a New York University Animal Welfare Committee (IACUC)-approved protocol. Available animals were assigned to treatment groups by using internal identification numbers without other identifying data.

Surgery and in vivo treatment with 405-nm light. All surgical procedures were performed between late morning and early afternoon, during the middle of the normal light cycle. Mice were anesthetized in a chamber containing 1.5% to 5% isoflurane (Forane, Baxter Healthcare, Deerfield, IL) and transferred to a surgical platform, where isoflurane was provided through a nose cone at 1.5% to 2% for the duration of surgery and treatment. Heat support from a circulating water blanket was provided during the procedure and recovery period. The surgical site was clipped and cleaned by using povidone–iodine and 70% isopropanol swabs. Aseptic surgical technique was used during the craniotomy procedure. A 2- to 3-cm rostral-to-caudal incision was made on the midline of the cranium, and the underlying tissue was cleared by using sterile cotton-tipped applicators. A burr-hole craniotomy (2 mm) was introduced by applying a

0.7-mm drill bit (Fine Science Tools, Foster City, CA) approximately 1 to 2 mm rostral to lambda and 1 to 2 mm lateral of midline. Burr holes were made in approximately the same position in each mouse to facilitate sectioning of that area for histopathology. Each mouse received 1 of 4 doses (0, 36, 45 or 54 J/cm² light treatment) at a distance of 5 cm, with the center of the light array over the surgical site (n = 21 per treatment group; n = 7 per treatment group were euthanized at 24 h, 72 h, and 21 d; Figure 2). Mice receiving light treatment were maintained on 1% to 2% isoflurane through a nose cone, as done during surgery. Skin was closed by using tissue glue (VetBond, 3M, Maplewood, MN), and all mice received a single dose of sustained-released buprenorphine (0.025 mg, approximately 1mg/kg; Zoopharm, Windsor, CO) subcutaneously before recovery. Animals were transferred to a recovery cage on a heating pad, monitored until full recovery, and then returned to their home cages. Mice were observed for neurologic signs (head tilt, difficulty ambulating, dullness, reluctance to move), wound dehiscence, or discomfort due to surgical manipulation daily for 3 d or until euthanasia, if sooner. Mice were observed daily for clinical signs of neurologic impairment or infection both by animal care staff (blinded to treatment) and the study team.

Tissue collection and processing. Mice were euthanized by CO_2 asphyxiation and subsequently perfused transcardially with 5 mL 4% paraformaldehyde solution. Brains were removed, fixed for 24 to 72 h at room temperature in 10% neutral buffered formalin (Neogen, Lansing, MI), and then moved to PBS (made from sodium mono- and dibasic phosphate, sodium chloride from Sigma-Aldrich, St Louis, MO; Fisher Scientific, Hampton, NH) for storage at 4 °C. Before being embedded, brains were washed with PBS and transferred to 70% ethanol. Tissues were embedded in paraffin by the New York University Langone Health Experimental Pathology Research Laboratory (tissue processor, Peloris II; embedder, model EG 1160; both from Leica, Wetzlar, Germany).

Brain histopathology staining, scoring, and interpretation. Paraffin-embedded brains were sectioned into 5-µm coronal sections, and 2 sections from each animal were stained with hematoxylin and eosin at Langone Health Experimental Pathology Research Laboratory (New York University) for histopathologic analysis. Each section included the cerebral cortical area below the craniotomy site and the contralateral side that was not drilled. Skull overlying brain of contralateral side was exposed to direct light, to serve as an internal control. Brains from 2 mice (randomized) from each treatment group were used for immunofluorescence analysis; 2 sections were stained form each specimen. Prior to immunofluorescence staining, location had been confirmed by visually locating the lesion location on histopathology slides. Stained slides were scanned (Aperio AT2, Leica) and analyzed by a board-certified veterinary pathologist (AM), who was blinded to treatment group. Lesions were planned to be scored according to a tissue-scoring system adapted from a study assessing the histologic effects of infrared pulses on the brain[8] as well as other sources describing brain injury and radiation necrosis.[16,24,30,31]

Immunohistochemical staining and interpretation. Glial fibrillary acidic protein was selected as a marker of astrocytes, and caspase 3 was selected as a marker of apoptosis.[4,24,30,31] Immunofluorescence analysis was performed on paraformaldehyde-fixed, paraffin-embedded, 5-µm coronal sections of murine brain by using unconjugated, mouse antiglial fibrillary acidic protein (clone cocktail 4A1, 1B4, 2E1; catalog no. 556330, lot no. 3172792, RRID AB_396368, BD Biosciences.) and unconjugated rabbit anticleaved caspase 3 (clone D3E9; catalog no. 9579, lot
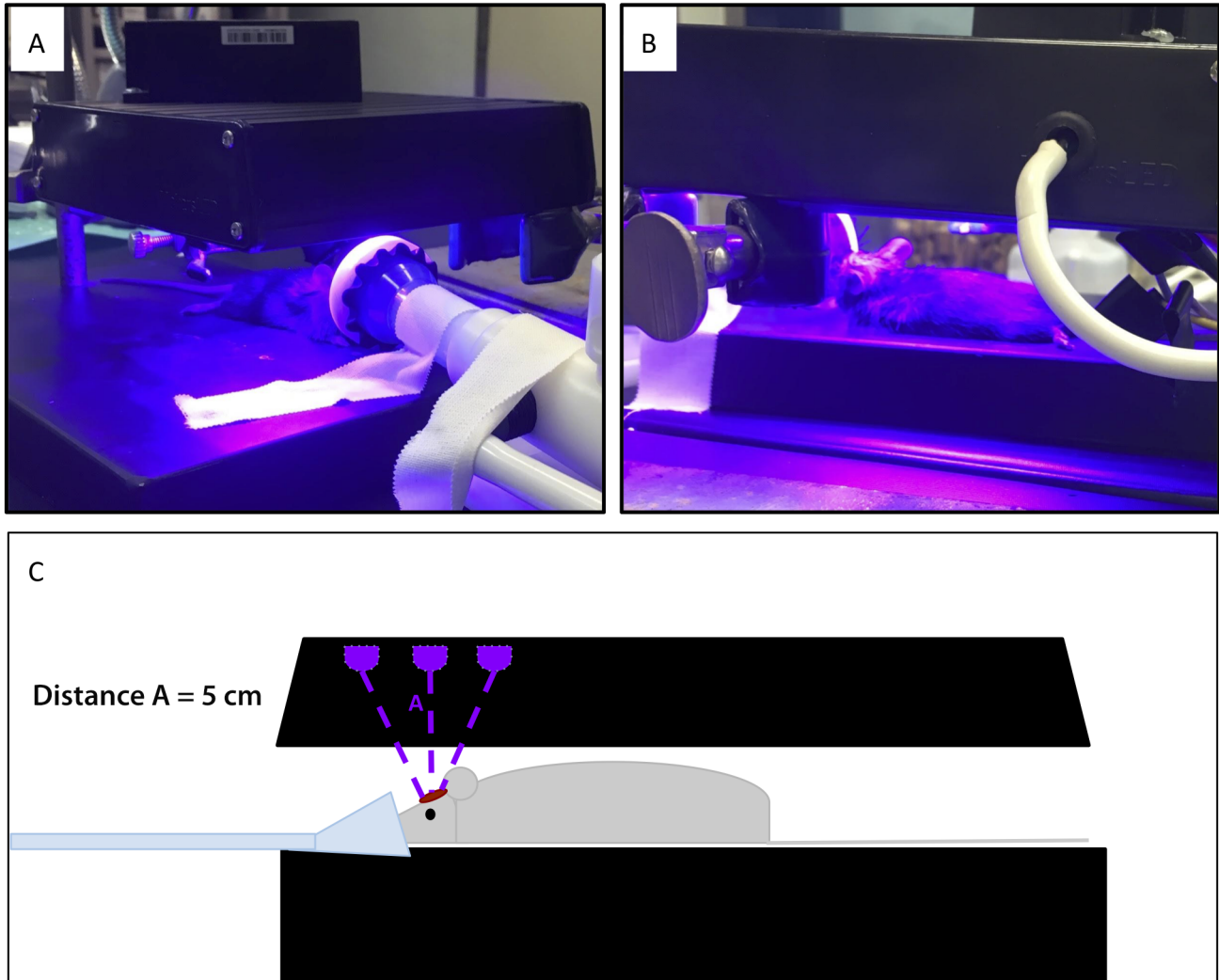
Figure 2. (A and B) Isoflurane-anesthetized mice receiving light treatment after craniotomy. (C) Drawing of the setup shown in panels A and B.

no. 1, RRID AB_10897512, Cell Signaling Technologies). Indirect immunofluorescence was performed on Discovery XT instrument (Ventana Medical Systems) with online deparaffinization by using the manufacturer's reagents and detection kits unless otherwise noted. Antigen retrieval was accomplished by using prediluted Cell Conditioner 1 (Tris, EDTA, and borate [pH8.5]; Ventana) for 20 min. Nonspecific protein interactions were blocked by using PBS containing 1% nonfat dry milk, 1% BSA, and 0.05% Tween 20 for 20 min. Antibodies to glial fibrillary acidic protein and cleaved caspase 3 were diluted 1:100 and 1:250, respectively, in Tris-buffered saline containing 1% BSA and incubated for 12 h at room temperature. Glial fibrillary acidic protein was detected by using Alexa-Fluor 555–conjugated donkey antimouse antibody (catalog no. A31570, lot no. 1850121, RRID AB_2536180, ThermoFisher Scientific), and cleaved caspase 3 was detected by using Alexa-Fluor 555–conjugated donkey antirabbit antibody (catalog no. A31572, lot no. 1891766, RRID AB_162543, ThermoFisher Scientific); both antibodies were diluted 1:100 in Tris-buffered saline containing 1% BSA and incubated for 1 h at 37.0 °C. Labeled slides were washed in distilled water, counterstained by using 100-ng/mL DAPI, and coverslipped with Prolong Gold Anti-Fade media (Molecular Probes). Appropriate positive and negative controls were included. Slides were generated and stained at Langone Health Experimental Pathology Research Laboratory (New York University) and analyzed by a board-certified pathologist (AM), who was blinded to treatment group.

Results

Device power and temperature. The array device was tested at 3 measured distances from the central LED of the 3×3 diode array, and the average power was 31.5 mW at 3 cm, 18.5 mW at 5 cm, and 13.0 mW at 6 cm; these data were converted to irradiance (power per unit area). Times were calculated to provide the desired doses (radiant exposure) of 54, 45, and 36 J/cm^2 at each distance (Table 1). Power regression of irradiance compared with distance yielded an R^2 value of 0.996, indicating the expected behavior of power measurement in adherence to the inverse-squares law.[12] Tissue surface temperature starting from room temperature did not exceed mammalian body temperature (38 °C, range: 36 to 38 °C) on exposure to the highest dose selected for testing.

Antimicrobial activity in vitro. The array device was tested on a dilute, pure *E. cloacae* clinical isolate in broth. Bacterial concentrations were determined through serial dilution, culture,

Table 1. Calculated exposure times (minutes) to deliver 3 doses selected because of their antimicrobial and mammalian-cell–sparing properties.

Distance (cm)	Measured irradiance (mW)	36 J/cm²	45 J/cm²	54 J/cm²
3	31.5	13.3	16.7	20.0
5	18.5	23.1	28.9	34.6
6	13.0	32.4	40.5	48.6

The calculated times are shown based on data transformed to mW/cm². The R^2 value of the linear regression of calculated irradiance (mW/cm²) compared with $1/r^2$ is 0.98 in agreement with the inverse-squares law. Power regression of irradiance compared with distance yielded an R^2 value of 0.996.

and counting and yielded data that were consistent with the expected dilution factor of 10. Cultures with 10^6 and 10^7 cfu/mL were exposed to 54, 45, and 36 J/cm² of light and counted at 24 h after plating, revealing a 10^4 order of magnitude attenuation of bacterial growth at the highest dose (Figure 3). According to 2-factor ANOVA, bacterial survival ($N:N_0$ ratio) was significantly ($P < 0.05$) affected by dose of exposure. By Tukey posthoc analysis, 45 and 56 J/cm² dose–response means were not significantly different from each other; all other comparisons were significant ($P < 0.05$).

Surgery and clinical outcomes. All mice recovered from surgery, but 2 animals were euthanized in the postoperative period: one for fighting, and one for incision dehiscence. No abnormal neurologic behavior, such as head tilt, dullness, or difficulty or unwillingness to ambulate, was noted during observation by animal care staff blinded to treatment groups, and all animals appeared comfortable and active until their euthanasia time point.

Histopathologic and immunohistochemical results. Analysis of brain sections stained with hematoxylin and eosin revealed no histopathologic changes related to the light exposure in the treatment groups (Figure 4). Staining patterns of glial fibrillary acidic protein and caspase 3 did not differ between the treatment groups (data not shown), thus corroborating the histopathologic finding.

Discussion

Low-power light therapy (phototherapy) is an emerging field of treatment. Antimicrobial light devices have been successful in vitro and for various clinical applications, such as burn wounds. In laboratory animal medicine, antimicrobial modalities that do not require pharmacologic intervention are of particular interest, particularly for study designs that may preclude antibiotic therapy or for treatment of infections in immunologically privileged sites, such as the brain. True-violet light therapy may represent a refinement in surgical and craniotomy site management, provide that its ability to kill surface bacteria in vitro is recapitulated in vivo. This consistency has previously been shown in a burn wound model and may hold true for other tissue surfaces.[9]

In the current study, we have extrapolated the function of light devices developed for environmental or wound decontamination to treat the murine brain after craniotomy. We were able to inexpensively build a device of appropriate power to deliver antimicrobial light treatment to the brains of mice, causing no observable tissue damage in excess of artifact caused by drilling during surgery. Histopathologic findings were supplemented by immunofluorescence staining for glial fibrillary acidic protein and caspase 3, markers of necrosis and apoptosis in the brain, which similarly were consistent across groups. We demonstrated antimicrobial efficacy of the device and mode of treatment in bacterial culture, recapitulating the work of previous studies with similar devices. Although we did not observe a
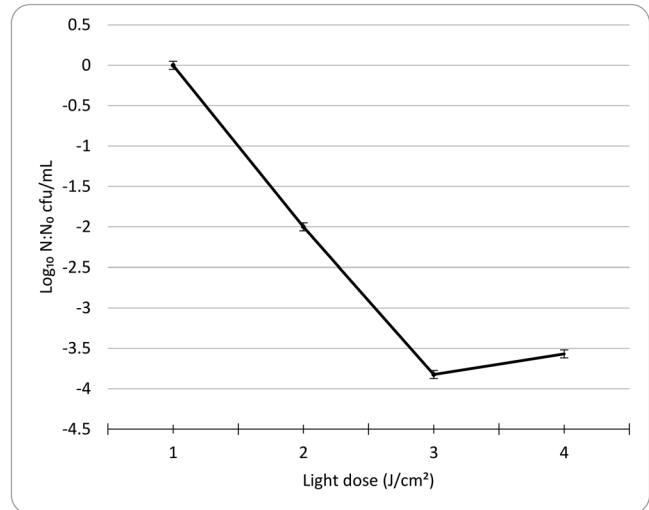

Figure 3. Mean logarithmic decrease in the $N:N_o$ ratio (no. of cfu after treatment: no. of cfu before treatment) of enumerated colony forming units of *Enterobacter cloacae* after 24-h incubation at 37 °C on tryptic soy agar after treatment in vitro with calculated doses of light. Error bars reflect 1 SD of log-transformed values.

strictly dose-dependent logarithmic decrease in bacterial count in vitro, the overall attenuation after light treatment was significant. Because the initial concentrations were selected to be near the limit of penetrable opacity for a device of this power, this situation may have affected the degree and pattern of attenuation observed. The in vitro activity of this type of device at multiple doses and against multiple clades has been well documented in the literature prior to this study. Of note, the bacterial isolate used in this study was a clinical isolate from a chronic infection in an NHP; this isolate was resistant to many antibiotics, including gentamicin, amikacin, enrofloxacin, ampicillin, and tetracycline (Idexx BioAnalytics results). These are the most commonly applied antibiotics in our facility and represent several distinct antibiotic classes. True-violet light therapy could represent a significant improvement to current management practices for chronic cephalic implant infections in NHP.

Several properties of visible light may make this treatment modality difficult to implement. The power delivered is related to the inverse square of the distance from the center of a diode, so time required to deliver an antimicrobial dose rises very quickly as the device is further from the area of treatment. Mounting a device closer to the area of interest may be possible, but that improvement could be negated by heat. We did not encounter clinical issues related to the temperature of the device, such as thermal damage to tissues, possibly because the array was mounted to a heatsink and was used from a distance of several centimeters from the animal. Surface temperatures did not exceed mammalian body temperature (38 °C), even after exposure to the highest studied dose. However, surface
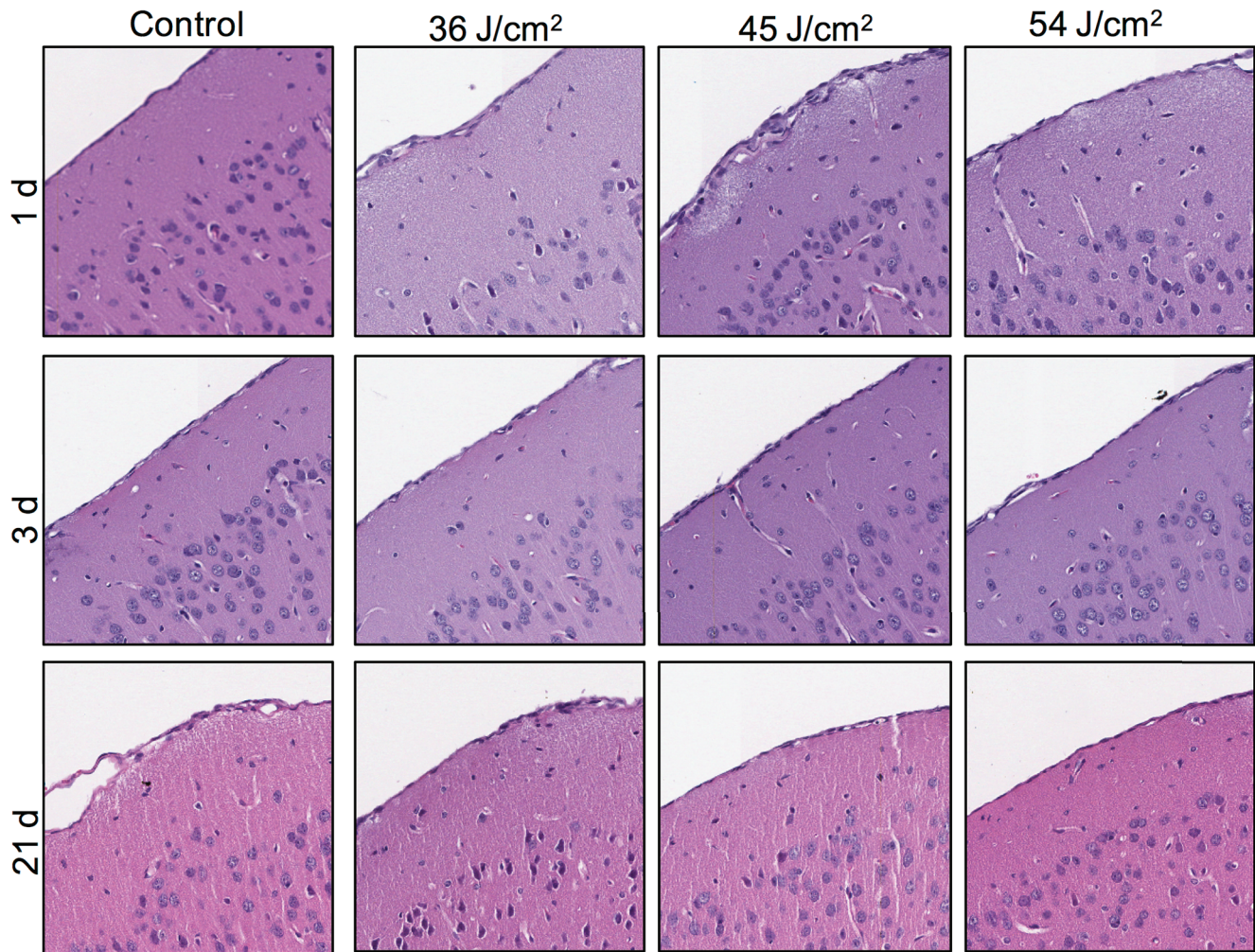
Figure 4. Coronal sections reveal no significant pathology in the mice euthanized at 1, 3, or 21 d after various doses of light treatment. Row and column headers refer to the treatment groups of the represented section. Each photomicrograph represents a different mouse. All sections are oriented at an angle, with the meninges along the diagonal from the lower-left to upper-right corner of the photograph. Cropped images were obtained from the area subjacent to the craniotomy site as confirmed at lower magnification. Hematoxylin and eosin stain; magnification, 10×.

temperatures should be considered if this device is adapted for translational use in other species. Light is stopped or heavily attenuated by passage through opaque or translucent material, so this type of visible light device would provide antimicrobial action against surface bacteria or dilute suspensions only. Despite this drawback, this treatment modality may still be useful against biofilms, at surgical sites, or after flushing of open craniotomy sites or chambers. In addition, maintaining the light source perpendicular to the surface is crucial to ensure that the calculated dosage is delivered; consequently precise positioning is very important. For clinical applications and if used near tissues, precise positioning and heat conduction would need to be addressed. However, given that similar devices at different wavelengths are already in use in the dermatology field, these adaptations should be feasible.

True-violet light therapy is associated with several clinical and research-related drawbacks. In neuroscience protocols, phototherapy could interfere with optogenetic studies, which usually use green or blue light to excite neurons of interest. Violet light is slightly higher in frequency but may still affect the fluorescence of target neurons. Perhaps this modality could still be used at the time of surgery or before exogenous fluorescent compounds are administered or expressed. In addition, light in the true-violet range may cause ocular damage, particularly if

the light is applied over a prolonged period of time to an anesthetized animal.[26] For repeated use of this modality, eye protection would need to be addressed or a barrier would need to be created between the light source and the animal's eye, to prevent clinical or welfare effects.

In vivo studies on bacterial inoculation of the craniotomy site would be valuable to further evaluate the clinical efficacy of a true-violet LED device. We did not assess tissue damage over time after multiple treatments; because repeated treatments may be more applicable to the clinical management of craniotomy sites than single exposures, further investigation beyond the scope of this study would be required to make conclusions regarding device safety after repeated use. We understand that translational application of true-violet phototherapy to the management of cephalic chambers in NHP may be the most clinically relevant in vivo application in laboratory animal medicine. However we chose mice as a model mammalian organism to demonstrate tissue safety after use of this modality at the brain surface. We also did not test safety or efficacy in large animal species, but application of true-violet light within the chamber or on the margins of cephalic implants should be considered, although brain surfaces with gyri may present more of a challenge for this modality than lissencephalic brain surfaces. Current results

support pursuing further studies of true-violet phototherapy in vivo as a way to treat bacterial contamination or infection in craniotomy sites.

Acknowledgments

References

1. **Abee C, Mansfield K, Tardif S, Morris T, editors.** 2012. Nonhuman primates in biomedical research, vol 2. London: Elsevier.

2. **Adams DL, Economides JR, Jocson CM, Parker JM, Horton JC.** 2011. A watertight acrylic-free titanium recording chamber for electrophysiology in behaving monkeys. J Neurophysiol **106:**1581–1590. https://doi.org/10.1152/jn.00405.2011.

3. **Association of Primate Veterinarians.** [Internet]. 2015.Cranial implant care guidelines for nonhuman primates in biomedical research. APV scientific advisory committee guidelines. [Cited 03 January 2017]. Available at: https://www.primatevets.org/guidance-documents

4. **Babaee A, Eftekhar-Vaghefi SH, Asadi-Shekaari M, Shahrokhi N, Soltani SD, Malekpour-Afshar R, Basiri M.** 2015. Melatonin treatment reduces astrogliosis and apoptosis in rats with traumatic brain injury. Iran J Basic Med Sci **18:**867–872.

5. **Bache SE, Maclean M, MacGregor SJ, Anderson JG, Gettinby G, Coia JE, Taggart I.** 2012. Clinical studies of the high-intensity narrow-spectrum light environmental decontamination system (HINS-light EDS), for continuous disinfection in the burn unit inpatient and outpatient settings. Burns **38:**69–76. https://doi.org/10.1016/j.burns.2011.03.008.

6. **Baxter D.** 2008. Low intensity laser therapy. In: Watson T, editor. Electrotherapy: evidence based practice. New York (NY): Elsevier.

7. **Cheng KP, Kiernan EA, Eliceiri KW, Williams JC, Watters JJ.** 2016. Blue light modulates murine microglial gene expression in the absence of optogenetic protein expression. Sci Rep **6:**1–11. https://doi.org/10.1038/srep21172.

8. **Chernov MM, Chen G, Roe AW.** 2014. Histological assessment of thermal damage in the brain following infrared neural stimulation. Brain Stimul **7:**476–482. https://doi.org/10.1016/j.brs.2014.01.006.

9. **Dai T, Gupta A, Huang YY, Yin R, Murray CK, Vrahas MS, Sherwood ME, Tegos GP, Hamblin MR.** 2012. Blue light rescues mice from potentially fatal *Pseudomonas aeruginosa* burn infection: efficacy, safety, and mechanism of action. Antimicrob Agents Chemother **57:**1238–1245. https://doi.org/10.1128/AAC.01652-12.

10. **Dai T, Gupta A, Murray CK, Vrahas MS, Tegos GP, Hamblin MR.** 2012. Blue light for infectious diseases: *Propionibacterium acnes, Helicobacter pylori*, and beyond? Drug Resist Updat **15:**223–236. https://doi.org/10.1016/j.drup.2012.07.001.

11. **Dashti SR, Baharvahdat H, Spetzler RF, Sauvageau E, Chang SW, Stiefel MF, Park MS, Bambakidis NC.** 2008. Operative intracranial infection following craniotomy. Neurosurg Focus **24:**E10. https://doi.org/10.3171/FOC/2008/24/6/E10.

12. **Gamry Instuments.** [Internet]. 2019. Measuring the optical power of your LED. [Cited 30 July 2019]. Available at: https://www.gamry.com/application-notes/instrumentation/measuring-optical-power-of-led/.

13. **Gillespie JB, Maclean M, Given MJ, Wilson MP, Judd MD, Timoshkin IV, MacGregor SJ.** 2017. Efficacy of pulsed 405-nm light-emitting diodes for antimicrobial photodynamic inactivation: effects of intensity, frequency, and duty cycle. Photomed Laser Surg **35:**150–156. https://doi.org/10.1089/pho.2016.4179.

14. **Gwynne PJ, Gallagher MP.** 2018. Light as a broad-spectrum antimicrobial. Front Microbiol **9:**119. https://doi.org/10.3389/fmicb.2018.00119.

15. **Huang Z, Ma J, Chen J, Shen B, Pei F, Kraus VB.** 2015. The effectiveness of low-level laser therapy for nonspecific chronic low back pain: a systematic review and meta-analysis. Arthritis Res Ther **17:**1–8. https://doi.org/10.1186/s13075-015-0882-0.

16. **Jortner BS.** 2006. The return of the dark neuron. A histologic artifact complicating contemporary neurotoxicologic evaluation. Neurotoxicology **27:**628–634. https://doi.org/10.1016/j.neuro.2006.03.002.

17. **Lee G, Danneman PJ, Rufo RD, Kalesnykas RP, Eng VM.** 1998. Use of chlorine dioxide for antimicrobial prophylactic maintenance of cephalic recording devices in rhesus macaques (*Macaca mulatta*). Contemp Top Lab Anim Sci **37:**59–63.

18. **Maclean M, Anderson JG, MacGregor SJ, White T, Atreya CD.** 2016. A new proof of concept in bacterial reduction: antimicrobial action of violet-blue light (405nm) in *Ex Vivo* stored plasma. J Blood Transfus **2016:**1–11. https://doi.org/10.1155/2016/2920514.

19. **Maclean M, MacGregor SJ, Anderson JG, Woolsey G.** 2009. Inactivation of bacterial pathogens following exposure to light from a 405-nanometer light-emitting diode array. Appl Environ Microbiol **75:**1932–1937. https://doi.org/10.1128/AEM.01892-08.

20. **Maclean M, McKenzie K, Anderson JG, Gettinby G, MacGregor SJ.** 2014. 405 nm light technology for the inactivation of pathogens and its potential role for environmental disinfection and infection control. J Hosp Infect **88:**1–11. https://doi.org/10.1016/j.jhin.2014.06.004.

21. **Maclean M, Anderson JG, Macgregor SJ.** [Internet]. 2015. New antimicrobial strategies appearing out of the blue. microbiology society. [Cited 03 January 2017]. Available at: https://microbiologysociety.org/publication/past-issues/light/article/new-antimicrobial-strategies-appearing-out-of-the-blue.html.

22. **Murdoch LE, Maclean M, Endarko E, MacGregor SJ, Anderson JG.** 2012. Bactericidal effects of 405nm light exposure demonstrated by inactivation of *Escherichia, Salmonella, Shigella, Listeria*, and *Mycobacterium* species in liquid suspensions and on exposed surfaces. ScientificWorldJournal **2012:**1–8. https://doi.org/10.1100/2012/137805.

23. **Ramakrishnan P, Maclean M, MacGregor SJ, Anderson JG, Grant MH.** 2016. Cytotoxic responses to 405nm light exposure in mammalian and bacterial cells: Involvement of reactive oxygen species. Toxicol In Vitro **33:**54–62. https://doi.org/10.1016/j.tiv.2016.02.011.

24. **Semple BD, Blomgren K, Gimlin K, Ferriero DM, Noble-Haeusslein LJ.** 2013. Brain development in rodents and humans: Identifying benchmarks of maturation and vulnerability to injury across species. Prog Neurobiol **106–107:**1–16. https://doi.org/10.1016/j.pneurobio.2013.04.001.

25. **R Foundation.** [Internet]. 2018. R: A language and environment for statistical computing. R Foundation for statistical computing. [Cited 28 January 2019]. Available at: https://www.R-project.org/.

26. **Walker DP, Vollmer-Snarr HR, Eberting CLD.** 2012. Ocular hazards of blue-light therapy in dermatology. J Am Acad Dermatol **66:**130–135. https://doi.org/10.1016/j.jaad.2010.11.040.

27. **Wang Y, Wu X, Chen J, Amin R, Lu M, Bhayana B, Zhao J, Murray CK, Hamblin MR, Hooper DC, Dai T.** 2016. Antimicrobial blue light inactivation of gram-negative pathogens in biofilms: in vitro and in vivo studies. J Infect Dis **213:**1380–1387. https://doi.org/10.1093/infdis/jiw070.

28. **Watson T.** [Internet]. 2018. Laser therapy. Electrotherapy on the web. [Cited 5 October 2018]. Available at: http://www.electrotherapy.org/modality/laser-therapy#Introduction.

29. **Woods SE, Lieberman MT, Lebreton F, Trowel E, de la Fuente-Núñez C, Dzink-Fox J, Gilmore MS, Fox JG.** 2017. Characterization of multi-drug resistant *Enterococcus faecalis* isolated from cephalic recording chambers in research macaques

(*Macaca* spp.). PLoS One **12:**1–20. https://doi.org/10.1371/journal.pone.0169293.

30. **Yoritsune E, Furuse M, Kuwabara H, Miyata T, Nonoguchi N, Kawabata S, Hayasaki H, Kuroiwa T, Ono K, Shibayama Y, Miyatake S.** 2014. Inflammation as well as angiogenesis may participate in the pathophysiology of brain radiation necrosis. J Radiat Res (Tokyo) **55:**803–811. https://doi.org/10.1093/jrr/rru017.

31. **Yoshii Y.** 2008. Pathological review of late cerebral radionecrosis. Brain Tumor Pathol **25:**51–58. https://doi.org/10.1007/s10014-008-0233-9.

32. **Zhang Y, Zhu Y, Chen J, Wang Y, Sherwood ME, Murray CK, Vrahas MS, Hooper DC, Hamblin MR, Dai T.** 2016. Antimicrobial blue light inactivation of Candida albicans: In vitro and in vivo studies. Virulence **7:**536–545. https://doi.org/10.1080/21505594.2016.1155015.